

# Multi-objective minimum time optimal control for low-thrust trajectory design

Nikolaus Vertovec

Sina Ober-Blöbaum

Kostas Margellos

**Abstract**—We propose a reachability approach for infinite and finite horizon multi-objective optimization problems for low-thrust spacecraft trajectory design. The main advantage of the proposed method is that the Pareto front can be efficiently constructed from the zero level set of the solution to a Hamilton-Jacobi-Bellman equation. We demonstrate the proposed method by applying it to a low-thrust spacecraft trajectory design problem. By deriving the analytic expression for the Hamiltonian and the optimal control policy, we are able to efficiently compute the backward reachable set and reconstruct the optimal trajectories. Furthermore, we show that any reconstructed trajectory will be guaranteed to be weakly Pareto optimal. The proposed method can be used as a benchmark for future research of applying reachability analysis to low-thrust spacecraft trajectory design.

## I. INTRODUCTION

Reachability analysis is an important research topic in the dynamics and control literature and has been used extensively for controller synthesis of complex systems [1], [2]. In recent years we have also seen the use of reachability theory to design controllers that keep the state of the system in a "safe" part of the state space while steering the system towards a target set. Typically, these approaches rely on the computation of a capture basin (i.e. the set of points from which the target set can be safely reached within a given finite time). Computing such capture basins using a Hamilton-Jacobi-Bellman (HJB) approach has been shown in [3]–[7]. In [8] the authors propose an extension of the HJB approach to solve an infinite horizon multi-objective optimization problem (MOP) with state space constraints. Intuitively, in a multi-objective optimal control problem, one seeks to find the minimum control effort way a dynamical system can perform a certain task, while minimizing or maximizing a set of, usually contradictory and incommensurable, objective functions [9]. A common example is found in spacecraft trajectory design, where the objective is to minimize the consumed propellant as well as transition time between two given orbits. However, since the final time is chosen as an optimization parameter, the approach described in [8] is no longer applicable. We, therefore, propose an extension that parameterizes the final time as an optimization variable by converting an infinite horizon control problem to a finite horizon one. The advantage of the proposed technique is that we are able to efficiently construct the Pareto front and optimal trajectories from the solution of a single HJB equation.

Nikolaus Vertovec and Kostas Margellos are with the University of Oxford. Email: {nikolaus.vertovec, kostas.margellos}@eng.ox.ac.uk. Sina Ober-Blöbaum is with the University of Paderborn. Email: {sinaober@math.uni-paderborn.de}.

This can make the comparison of multiple trajectories vastly more efficient compared with typical shooting methods [10]. This paper is organized into five sections. Section II contains details regarding the derivations of the spacecraft dynamics as well as the definitions of the constraints pertaining its behavior. In Section III the optimal control problem is formulated and the set of optimal trajectories is derived from the unique viscosity solution of a HJB equation. Section IV summarizes the simulation results obtained and discusses the numerical implementation. Finally, Section V provides concluding remarks and directions for future work. Most of the proofs have been omitted, but can be found in the extended version of the paper [11].

## II. MODELING

### A. Spacecraft equations of motion

The spacecraft thrust can be modeled using the input  $\mathbf{u}(t) := [\mathbf{u}_x(t), \mathbf{u}_y(t), \mathbf{u}_z(t)]^T \in \mathcal{U}$  where  $\mathcal{U}$  is the set of possible control inputs.  $\mathbf{u} \in \mathcal{U}_{ad}$  denotes the control policy and  $\mathcal{U}_{ad}$  denotes the set of admissible policies which is the set of Lebesgue measurable functions from  $[0, +\infty]$  to  $\mathcal{U}$ . Boldface notation is used to denote trajectories and non boldface notation is used to denote scalars and vectors.

The equations of motion of a particle or spacecraft around a rotating body can be expressed in 3-dimensional Euclidean space as a second-order ordinary differential equation [12]

$$2\boldsymbol{\Omega}(t) \times \frac{\partial \mathbf{R}(t)}{\partial t} + \boldsymbol{\Omega}(t) \times (\boldsymbol{\Omega}(t) \times \mathbf{R}(t)) + \frac{\partial U(\mathbf{R}(t))}{\partial \mathbf{R}} + \frac{\partial \boldsymbol{\Omega}(t)}{\partial t} \times \mathbf{R}(t) - \frac{\mathbf{u}(t)}{m(t)} = -\frac{\partial^2 \mathbf{R}(t)}{\partial t^2}, \quad (\text{II.1})$$

where  $\mathbf{R}(t)$  is the radius vector from the asteroids center of mass to the particle, the first and second time derivatives of  $\mathbf{R}(t)$  are with respect to the body-fixed coordinate system,  $U(\mathbf{R}(t))$  is the gravitational potential of the asteroid and  $\boldsymbol{\Omega}$  is the rotational angular velocity vector of the asteroid relative to inertial space. We consider an asteroid rotating uniformly with constant magnitude  $\omega$  around the  $z$ -axis. Therefore, the euler forces  $\frac{\partial \boldsymbol{\Omega}(t)}{\partial t} \times \mathbf{R}(t)$  can be neglected and we can express the rotation vector as  $\boldsymbol{\Omega} := \omega \cdot e_z$ , where  $e_z$  is the unit vector along the  $z$ -axis. Following [13], the radius vector and its derivatives are given by  $\mathbf{R}(t) := [\mathbf{x}(t), \mathbf{y}(t), \mathbf{z}(t)]^T$ ,  $\frac{\partial \mathbf{R}(t)}{\partial t} = [\mathbf{v}_x(t), \mathbf{v}_y(t), \mathbf{v}_z(t)]^T$ . The coriolis and centrifugal forces

(the first two terms in (II.1)) acting on the spacecraft are

$$2\Omega \times \frac{\partial \mathbf{R}(t)}{\partial t} = \begin{bmatrix} -2\omega \mathbf{v}_y(t) \\ 2\omega \mathbf{v}_x(t) \\ 0 \end{bmatrix}, \Omega \times (\Omega \times \mathbf{R}(t)) = \begin{bmatrix} -\omega^2 \mathbf{x}(t) \\ -\omega^2 \mathbf{y}(t) \\ 0 \end{bmatrix}. \quad (\text{II.2})$$

Let us define the state vector  $r := [x, y, z, v_x, v_y, v_z, m]^T \in \mathbb{R}^7$ . Then following our derivations from (II.1) we can formulate the system dynamics of the spacecraft as

$$\dot{r} = \tilde{f}(r, u) = \begin{bmatrix} v_x \\ v_y \\ v_z \\ U_x(x, y, z) + \omega^2 x + 2\omega v_y + \frac{u_x}{m} \\ U_y(x, y, z) + \omega^2 y - 2\omega v_x + \frac{u_y}{m} \\ U_z(x, y, z) + \frac{u_z}{m} \\ -\frac{\sqrt{u_x^2 + u_y^2 + u_z^2}}{v_{\text{exhaust}}} \end{bmatrix}, \quad (\text{II.3})$$

where  $v_{\text{exhaust}}$  is the exhaust velocity,  $U_x$ ,  $U_y$  and  $U_z$  are the derivatives of the gravitational potential in the direction  $e_x$ ,  $e_y$  and  $e_z$ , respectively and where for brevity we neglect the time dependence by denoting  $r = \mathbf{r}(t)$ ,  $v_x = \mathbf{v}_x(t)$  etc.

### B. State constraints

In order to ensure that the derived spacecraft dynamics hold, we need to enforce state constraints on  $x, y, z$  as well as on the mass  $m$ .

Assuming that the burnout mass of the spacecraft is the same as the dry mass, then the total mass of the spacecraft is bounded by the amount of propellant available. We set  $m_{\min} := m_{\text{dry}}$  and  $m_{\max} := m_{\text{dry}} + m_{\text{propellant}}$ . Since using all the propellant is never physically possible  $m_{\min}$  is formulated as a strict inequality.

Due to particles ejected from the asteroid, we do not want to fall below a circular orbit with radius  $\rho := \sqrt{x^2 + y^2 + z^2}$  of approximately  $\rho_{\min} = 1$  km. Furthermore, we need to stay within the sphere of influence (SOI) of the asteroid.

The SOI can be approximated by  $\rho_{\text{SOI}} \approx a \left( \frac{M_1}{M_2} \right)^{\frac{2}{5}}$ , where  $a$  is the semi-major axis of the asteroid's orbit around the sun ( $1.5907 \cdot 10^8$  km),  $M_1$  is the Mass of the asteroid ( $1.4091 \cdot 10^{12}$  kg) and  $M_2$  is the mass of the sun ( $1.9890 \cdot 10^{30}$  kg). Therefore, the sphere of influence of the asteroid is approximately  $\rho_{\max} = 8.74$  km. Let us denote the set of states that satisfy the above assumptions as

$$\mathcal{K}_0 := \{r \in \mathbb{R}^7 : \rho \in [\rho_{\min}, \rho_{\max}], m \in (m_{\min}, m_{\max}]\},$$

and let  $\overline{\mathcal{K}_0}$  denote the closure of  $\mathcal{K}_0$  and  $\mathcal{K}_0^\circ$  the interior.

Whenever we approach the boundary of  $\mathcal{K}_0$ , we wish to be able to recover and reenter the interior  $\mathcal{K}_0^\circ$ . We, therefore, restrict ourselves to the set  $\mathcal{K} := \{r \in \mathcal{K}_0 | \exists u \in \mathcal{U} : f(r, u) \cdot \eta_r < 0\}$ , where  $\eta_r$  is the exterior normal vector to  $\mathcal{K}$  at  $r$ . Recall that this need not hold for  $m = m_{\min} \notin \mathcal{K}_0$ . Overall, the set of state constraints we consider is encoded by the set  $\mathcal{K}$ , while the target orbit that we would like to transfer to lies within the nonempty closed target set  $\mathcal{C} \subset \mathcal{K}$  defined as  $\mathcal{C} := \{r \in \mathcal{K} : |r_{\text{target}} - r| < \epsilon\}$ , where  $\epsilon > 0$  is an arbitrary tolerance.

## III. OPTIMAL CONTROL PROBLEM

The multi-objective optimal control problem can be formulated as a minimization problem using two objective functions in Mayer form. The first goal is to maximize the remaining mass, the second minimizes the required time for the orbit change, i.e. the terminal time. However, as the terminal time  $t_f$  is unknown, we introduce a change of the time variable, i.e. for every  $t_f \in [0, +\infty)$ :

$$t_{t_f}(s) := t_0 + s(t_f - t_0) \quad \text{for } s \in [0, 1].$$

The new dynamics of the fixed final horizon problem (where the final horizon is 1 and  $t_0 := 0$ ) are then as follows:

$$\begin{aligned} f(r, u, t_f) &= (t_f - t_0) \tilde{f}(r, u) \\ \Rightarrow \begin{cases} \dot{\mathbf{r}}(s) = f(\mathbf{r}(s), \mathbf{u}(s), \zeta(s)) & s \in [\kappa, 1] \\ \dot{\zeta}(s) = 0 & s \in [\kappa, 1] \\ \mathbf{r}(\kappa) = r_0 \\ \zeta(\kappa) = t_f \end{cases}, \quad (\text{III.1}) \end{aligned}$$

where  $\kappa$  is chosen from  $[0, 1]$  and  $r_0$  is an initial state. The solution  $\mathbf{r}$  belongs to the Sobolev space  $\mathbb{W}^{1,1}([\kappa, 1]; \mathbb{R}^7)$ . The set of trajectory-control pairs on  $[0, 1]$  starting at  $r_0$  with terminal time  $t_f$  is denoted as:

$$\begin{aligned} \Pi_{r_0, t_f} &:= \{(\mathbf{r}, \mathbf{u}) : \dot{\mathbf{r}}(s) = f(\mathbf{r}(s), \mathbf{u}(s), \zeta(s)), s \in [0, 1]; \\ &\quad \mathbf{r}(0) = r_0, \zeta(0) = t_f\} \subset \mathbb{W}^{1,1}([0, 1]; \mathbb{R}^7) \times \mathcal{U}_{ad}. \end{aligned}$$

Similarly, the set of admissible (in the sense of satisfying the state constraints) trajectory-control pairs on  $[0, 1]$  starting at  $r_0$  with terminal time  $t_f$  is denoted as:

$$\begin{aligned} \Pi_{r_0, t_f}^{\mathcal{K}, \mathcal{C}} &:= \{(\mathbf{r}, \mathbf{u}) \in \Pi_{r_0, t_f} : \mathbf{r}(s) \in \mathcal{K} \text{ for } s \in [0, 1]; \\ &\quad \mathbf{r}(1) \in \mathcal{C}\} \subset \mathbb{W}^{1,1}([0, 1]; \mathbb{R}^7) \times \mathcal{U}_{ad}. \end{aligned}$$

Using Assumption 3.1 and 3.2 that will be defined in Section III-B, as well as Filippov's Theorem [14], we can conclude, that  $\Pi_{r_0, t_f}^{\mathcal{K}, \mathcal{C}}$  is compact.

Finally, the set of admissible terminal time and state pairs is denoted as

$$\pi := \{(r_0, t_f) \in \mathcal{K} \times [0, +\infty) \text{ such that } \Pi_{r_0, t_f}^{\mathcal{K}, \mathcal{C}} \neq \emptyset\}.$$

For a given terminal state  $r_f \in \mathbb{R}^7$  and terminal time  $t_f \in [0, +\infty)$ , we can define the costs functions as  $J_1(r_f, t_f) := -r_{f7}$  and  $J_2(r_f, t_f) := t_f$ , where  $r_{f7}$  denotes the 7th element of the state vector  $r_f$  (the mass in our case). The 2-dimensional objective function  $J : \mathbb{R}^7 \times [0, +\infty) \rightarrow \mathbb{R}^2$  can then be written as  $J(r_f, t_f) := [J_1(r_f, t_f), J_2(r_f, t_f)]$ .

We are now in a position to formulate the multi-objective optimal control problem (MOC) under study by

$$\begin{cases} \inf J(\mathbf{r}(1), t_f) \\ t_f \in [0, +\infty) \\ (\mathbf{r}, \mathbf{u}) \in \Pi_{r_0, t_f}^{\mathcal{K}, \mathcal{C}}. \end{cases} \quad (\text{III.2})$$

### A. Pareto Optimality

Before discussing how to solve (III.2), we will introduce two important concepts that are relevant when discussing multi-objective optimization. The first will be that of dominance between two admissible control pairs and the second will be weak and strong Pareto optimality [15].

*Definition 3.1:* A vector  $a$  is considered less than  $b$  (denoted  $a < b$ ) if for every element  $a_i$  and  $b_i$  the relation  $a_i < b_i$  holds. The relations  $\leq, \geq, >$  are defined in an analogous way.

*Definition 3.2:* Let  $(r_0, t_f), (r_0, \hat{t}_f) \in \pi$ . We consider the trajectory-control pairs  $(\mathbf{r}, \mathbf{u}) \in \Pi_{r_0, t_f}^{\mathcal{K}, \mathcal{C}}$  and  $(\mathbf{x}, \mathbf{v}) \in \Pi_{r_0, \hat{t}_f}^{\mathcal{K}, \mathcal{C}}$ .

- 1) The trajectory  $\mathbf{r}$  dominates  $\mathbf{x}$  if  $J(\mathbf{r}(1), t_f) \leq J(\mathbf{x}(1), \hat{t}_f)$  and  $J(\mathbf{r}(1), t_f) \neq J(\mathbf{x}(1), \hat{t}_f)$ .
- 2) The trajectory  $\mathbf{r}$  strictly dominates  $\mathbf{x}$  if  $J(\mathbf{r}(1), t_f) < J(\mathbf{x}(1), \hat{t}_f)$ .

*Definition 3.3:* Let  $(r_0, t_f) \in \pi$ . We consider the trajectory-control pairs  $(\mathbf{r}, \mathbf{u}) \in \Pi_{r_0, t_f}^{\mathcal{K}, \mathcal{C}}$ .

- 1) The trajectory  $\mathbf{r}$  is considered weakly Pareto optimal if  $\forall \hat{t}_f \in [0, \infty), \nexists (\mathbf{x}, \mathbf{v}) \in \Pi_{r_0, \hat{t}_f}^{\mathcal{K}, \mathcal{C}}$  such that  $J(\mathbf{x}(1), \hat{t}_f) < J(\mathbf{r}(1), t_f)$ .
- 2) The trajectory  $\mathbf{r}$  is considered strictly Pareto optimal if  $\forall \hat{t}_f \in [0, \infty), \nexists (\mathbf{x}, \mathbf{v}) \in \Pi_{r_0, \hat{t}_f}^{\mathcal{K}, \mathcal{C}}$  such that  $J(\mathbf{x}(1), \hat{t}_f) \leq J(\mathbf{r}(1), t_f)$ .

Following Definition 3.3, a trajectory  $\mathbf{r}$  is considered weakly Pareto optimal if it is not possible to improve all its performance metrics  $J_1(\mathbf{r}(1), t_f), J_2(\mathbf{r}(1), t_f)$  simultaneously. On the other hand, a trajectory  $\mathbf{r}$  is considered strongly Pareto optimal if no other admissible trajectory can ameliorate its performance metrics  $J_1(\mathbf{r}(1), t_f), J_2(\mathbf{r}(1), t_f)$  without deteriorating the other.

Letting  $(\mathbf{r}, \mathbf{u}) \in \Pi_{r_0, t_f}^{\mathcal{K}, \mathcal{C}}$  and  $z := \begin{pmatrix} z_1 \\ z_2 \end{pmatrix} \in \mathbb{R}^2$ , we now study how we can reconstruct Pareto optimal trajectories. First, we will choose a value function  $\vartheta : \mathbb{R}^7 \times \mathbb{R}^2 \rightarrow \mathbb{R}$ , discussed further in Section III-B, such that for any  $t_f \in [0, \infty)$  the following holds:

$$\vartheta(r_0, z) \leq 0 \iff \left[ \exists (\mathbf{r}, \mathbf{u}) \in \Pi_{r_0, t_f}^{\mathcal{K}, \mathcal{C}}, J_1(\mathbf{r}(1), t_f) \leq z_1 \text{ and } J_2(\mathbf{r}(1), t_f) \leq z_2 \right], \quad (\text{III.3})$$

$$\forall z, z' \in \mathbb{R}^2, z \leq z' \Rightarrow \vartheta(r_0, z) \geq \vartheta(r_0, z'). \quad (\text{III.4})$$

To discuss the following theorem, we introduce the utopian point  $J^*(r_0)$ , which is the lower bound of  $J$ , defined elementwise as

$$J_i^*(r_0) := \inf_{\{(\mathbf{r}(1), t_f) \mid \exists t_f : (r_0, t_f) \in \pi; (\mathbf{r}, \mathbf{u}) \in \Pi_{r_0, t_f}^{\mathcal{K}, \mathcal{C}}\}} J_i(\mathbf{r}(1), t_f). \quad (\text{III.5})$$

Furthermore, for the remainder of the paper,  $a \vee b$  will denote  $\max(a, b)$  and  $\bigvee_i x_i$  will denote the maximum element of the vector  $x$ .

*Theorem 3.1:* Let  $z_1^*(r_0)$  and  $z_2^*(r_0)$  be the two utopian values of  $J_1$  and  $J_2$  for a given initial state  $r_0$  and let us

define  $z^*(r_0) := \begin{pmatrix} z_1^*(r_0) \\ z_2^*(r_0) \end{pmatrix}$  and  $\mu := \begin{pmatrix} \mu_1 \\ \mu_2 \end{pmatrix} \in \mathbb{R}_{\geq 0}^2$ . Moreover, let  $\Pi_{r_0, z^*(r_0)}^{\mathcal{K}, \mathcal{C}} \neq \emptyset$ . We consider the extended function  $\Theta_{r_0} : [0, 1]^2 \rightarrow [0, \infty]$  defined as follows:

$$\Theta_{r_0}(\mu) := \inf \left\{ \tau \geq 0 \mid \vartheta(r_0, z^*(r_0) + \mu\tau) \leq 0 \text{ and } \tau < \frac{m_{\text{propellant}}}{\mu_1} \right\} \in [0, \infty].$$

Let us define the 1-dimensional manifold:

$$\Sigma_{r_0} := \left\{ \begin{pmatrix} z_1^*(r_0) \\ z_2^*(r_0) \end{pmatrix} + \mu \cdot \Theta_{r_0}(\mu), \mu := \begin{pmatrix} \mu_1 \\ \mu_2 \end{pmatrix} \in [0, 1]^2 \text{ with } \mu_1 + \mu_2 = 1 \right\}.$$

Any trajectory reconstructed from  $\Sigma_{r_0}$ , is guaranteed to be weakly Pareto optimal.

Since weak Pareto optimality is of less relevance compared to strong Pareto optimality, we make the following observation.

*Lemma 3.1:* The set of Pareto optimal values  $z$ , called the Pareto front  $\mathcal{F}$ , is a subset of  $\Sigma_{r_0}$ .

Following Lemma 3.1, we can construct the Pareto front from  $\Sigma_{r_0}$  by eliminating all points from  $\Sigma_{r_0}$  that are dominated. For a discretized approximation of  $\Sigma_{r_0}$ , this can be done by iteratively removing any point  $z$  that is dominated. Thus in conclusion, using the value function  $\vartheta$ , we are able to determine Pareto optimal solutions by constructing the set  $\Sigma_{r_0}$  and simply eliminating dominated points.

### B. Auxiliary value function

We now describe how the value function  $\vartheta$  and the set  $\Sigma_{r_0}$  can be computed. First, let  $g(r)$  and  $\nu(r)$  be two Lipschitz functions (with Lipschitz constants  $L_g$  and  $L_\nu$ , respectively) chosen such that

$$g(r) \leq 0 \iff r \in \bar{\mathcal{K}}, \\ \nu(r) \leq 0 \iff r \in \mathcal{C}.$$

This can be achieved by choosing  $g(r)$  and  $\nu(r)$  as signed distances to the sets  $\mathcal{K}$  and  $\mathcal{C}$ , respectively. Then, by letting  $(\mathbf{r}, \mathbf{u}) \in \Pi_{r_0, t_f}^{\mathcal{K}, \mathcal{C}}$  and  $z := \begin{pmatrix} z_1 \\ z_2 \end{pmatrix} \in \mathbb{R}^2$ , we can describe the epigraph of the MOC problem, as defined in (III.2), by using the auxiliary value function  $\omega$ :

$$\omega(\kappa, r_0, z, t_f) := \inf_{(\mathbf{r}, \mathbf{u}) \in \Pi_{r_0, t_f}} \left\{ \bigvee_i J_i(\mathbf{r}(1), t_f) - z_i \bigvee \nu(\mathbf{r}(1)) \bigvee \max_{s \in [\kappa, 1]} g(\mathbf{r}(s)) \right\}. \quad (\text{III.6})$$

Since,  $\omega(\kappa, r_0, z, t_f) \leq 0$  implies that we have found an admissible trajectory that remains within  $\bar{\mathcal{K}}$ , by limiting  $z_1$  to  $z_1 < -m_{\min}$  it follows that:

$$0 \geq \omega(\kappa, r_0, z, t_f) \geq J_1(\mathbf{r}(1), t_f) - z_1 = -m_{\text{final}} - z_1 \\ \iff m_{\text{final}} \geq -z_1 > m_{\min},$$

and thus the solution  $\mathbf{r}$  lies within  $\mathcal{K}$ .

For the following theorem, we need to make two assumptions about the spacecraft dynamics.

*Assumption 3.1:* For every  $r \in \bar{\mathcal{K}}$  the set  $\{\tilde{f}(r, u) : u \in \mathcal{U}\}$  is a compact convex subset of  $\mathbb{R}^7$ .

*Assumption 3.2:*  $\tilde{f} : \mathcal{K} \times \mathcal{U} \rightarrow \mathbb{R}^7$  is bounded and there exists an  $L_f > 0$  such that for every  $u_1, u_2 \in \mathcal{U}$ ,

$$|\tilde{f}(r_1, u_1) - \tilde{f}(r_2, u_2)| \leq L_f |r_1 - r_2|.$$

Moreover, following Assumption 3.1 there exists a  $c_f > 0$  such that for any  $r \in \bar{\mathcal{K}}$  we have  $\max\{|\tilde{f}(r, u)| : u \in \mathcal{U}\} \leq c_f(1 + |r|)$ .

Under Assumption 3.2 and following the Picard-Lindelöf theorem, for any control policy  $\mathbf{u} \in \mathcal{U}_{ad}$ , any initial starting orbit  $r \in \bar{\mathcal{K}}$  and terminal time  $t_f \geq 0$ , the system admits a unique, absolutely continuous solution on  $[0, t_f]$  [16]. By introducing the Hamiltonian  $H : \mathbb{R}^7 \times \mathbb{R} \times \mathbb{R}^7 \rightarrow \mathbb{R}$

$$H(r, t_f, q) := \min_{u \in \mathcal{U}} (q^T \cdot f(r, u, t_f)),$$

we are able to now state how the auxiliary value function can be obtained.

*Theorem 3.2:* The auxiliary value function  $\omega$  is the unique viscosity solution of the following HJB equation

$$\begin{cases} \min(\partial_\kappa \omega + H(r, t_f, \nabla_r \omega), \omega(\kappa, r, z, t_f) - g(r)) = 0 \\ \text{for } \kappa \in [0, 1], r \in \mathcal{K}, z \in \mathbb{R}^2, t_f \in [0, +\infty), \\ \omega(1, r, z, t_f) = \left( -r_7 - z_1 \sqrt{t_f - z_2} \sqrt{\nu(r)} \sqrt{g(r)} \right) \\ \text{for } r \in \mathcal{K}, z \in \mathbb{R}^2, t_f \in [0, +\infty), \end{cases}$$

Since the Dynamic Programming Principle holds for  $0 \leq \kappa \leq \kappa + h \leq 1$ ,  $r_0 \in \mathcal{K}$  and  $z \in \mathbb{R}^2$  with  $h \geq 0$ :

$$\omega(\kappa, r_0, z, t_f) = \inf_{(r, \mathbf{u}) \in \Pi_{r_0, t_f}} \left\{ \omega(\kappa + h, \mathbf{r}(\kappa + h), z, t_f) \vee \max_{s \in [\kappa, \kappa + h]} g(\mathbf{r}(s)) \right\},$$

the proof of Theorem 3.2 follows standard arguments for viscosity solutions, as shown in [3]. We will subsequently make some observations about the auxiliary value function  $\omega$ .

*Proposition 3.1:* The auxiliary value function  $\omega$  is Lipschitz continuous.

The proof of this Proposition follows from [17] and can be found in [11].

*Proposition 3.2:* Let  $(\kappa, r_0, t_f) \in [0, 1] \times \mathbb{R}^7 \times [0, +\infty)$ . The function  $\omega(\kappa, r_0, z, t_f)$  has the following property:

$$\forall z, z' \in \mathbb{R}^2, z \leq z' \Rightarrow \omega(\kappa, r_0, z, t_f) \geq \omega(\kappa, r_0, z', t_f).$$

*Proof:* Let  $(\kappa, r_0, t_f) \in [0, 1] \times \mathbb{R}^7 \times [0, +\infty)$  and  $z, z' \in \mathbb{R}^2$  with  $z \leq z'$ . Then for all  $i \in 1, 2$ ,  $J_i(\mathbf{r}(1), t_f) - z_i' \leq J_i(\mathbf{r}(1), t_f) - z_i$ , and consequently

$$\left[ \bigvee_i J_i(\mathbf{r}(1), t_f) - z_i' \right] \leq \left[ \bigvee_i J_i(\mathbf{r}(1), t_f) - z_i \right].$$

Taking the maximum  $\nu(\mathbf{r}(1)) \vee \max_{s \in [\kappa, 1]} g(\mathbf{r}(s))$  and the infimum over all  $(\mathbf{r}, \mathbf{u}) \in \Pi_{r_0, t_f}$ , it follows from the last equation that  $\omega(\kappa, r_0, z', t_f) \leq \omega(\kappa, r_0, z, t_f)$ . ■

We now use the auxiliary value function  $\omega$  to define  $\vartheta$  and show that  $\vartheta$  satisfies the requirements given in Section III-A.

$$\vartheta(r_0, z) := \min_{t_f} \omega(0, r_0, z, t_f).$$

*Lemma 3.2:* Let  $r_0 \in \mathbb{R}^7$ . Then  $\forall z, z' \in \mathbb{R}^2, z \leq z' \Rightarrow \vartheta(r_0, z) \geq \vartheta(r_0, z')$ .

Having shown how to construct  $\vartheta$  from the solution of a HJB equation, we are now in the position to state and prove the following theorem, which is the main result of this section.

*Theorem 3.3:*  $\Sigma_{r_0}$  is defined by the zero level set of the value function  $\vartheta$ , i.e.,  $\Sigma_{r_0} = \{z \in \mathbb{R}^2 | \vartheta(r_0, z) = 0\}$ .

## IV. NUMERICAL APPROXIMATION AND RESULTS

### A. Numerical approximation of $\omega$

Ultimately, the goal is to compute the set  $\Sigma_{r_0}$  and the corresponding optimal trajectories. First, however, we will need to discuss how  $\omega$  is computed from the HJB equation given in Theorem 3.2. Since the term  $J_2(\mathbf{r}(1), t_f) - z_2$  does not depend on the system dynamics, we can omit it from the initial condition of the auxiliary value function  $\omega$ , and simply take the maximum of  $\omega(0, r_0, z, t_f)$  and  $J_2(\mathbf{r}(1), t_f) - z_2$  to obtain the original  $\omega(0, r_0, z, t_f)$ , had  $J_2(\mathbf{r}(1), t_f) - z_2$  been included in the initial condition. This approach stems from an idea of system decomposition presented in [18] and allows us, for the sake of solving the HJB equation, to omit one grid dimension,  $z_2$ . To solve the HJB equation we need to consider a uniform spaced grid  $\mathcal{G} = \{r, z_1, t_f\}$  on  $\mathcal{K} \times \mathbb{R} \times [0, +\infty)$ , which enables us to use the Level Set Toolbox described in [19] as well as some extensions presented in [20].

Numerical results have shown that by sufficiently constraining the considered grid points, we get an acceptable approximation of the set  $\mathcal{K}$ . Since  $\mathcal{K}_0$  constrains the radius  $\rho$ , it is more efficient to compute the auxiliary value function  $\omega$  in spherical coordinates. Let us define  $[a_\rho, a_\theta, a_\psi]^T$  as the appropriate transformation of  $a_x := U_x(x, y, z) + \omega^2 x + 2\omega v_y$ ,  $a_y := U_y(x, y, z) + \omega^2 y - 2\omega v_x$  and  $a_z := U_z(x, y, z)$ . Then we can restate the system dynamics in spherical coordinates as

$$\dot{\mathbf{r}} = \begin{bmatrix} v_\rho \\ v_\theta \\ v_\psi \\ a_\rho + \frac{T}{m} \cos \alpha \\ a_\theta + \frac{T}{m} \sin \alpha \sin \delta \\ a_\psi + \frac{T}{m} \sin \alpha \cos \delta \\ -\frac{T}{v_{\text{exhaust}}} \end{bmatrix}, \quad (\text{IV.1})$$

where  $v_\rho$ ,  $v_\theta$  and  $v_\psi$  are the velocities in the direction  $e_r$ ,  $e_\theta$  and  $e_\psi$ , respectively. The input  $\mathbf{u}(t)$  is redefined for spherical coordinates as  $\mathbf{u}_{\text{sph}}(t) := (\boldsymbol{\alpha}(t), \boldsymbol{\delta}(t), \mathbf{T}(t)) \in \mathcal{U}$ , where  $\boldsymbol{\alpha}(t) \in [-\pi, \pi]$  is the incidence angle,  $\boldsymbol{\delta}(t) \in [-\frac{\pi}{2}, \frac{\pi}{2}]$  is the sideslip angle and  $\mathbf{T}(t) \in [0, T_{\text{max}}]$  is the variable thrust.

To obtain a numerical approximation of  $\omega$ , we use a Lax-Friedrich Hamiltonian with an appropriate fifth-order weighted essentially non-oscillatory scheme as detailed in [21]. As the PDE is solved backwards in time using a finite difference scheme, the Hamiltonian is given by  $H(r, q) := -\min_{u \in \mathcal{U}} (f(r, u, t_f) \cdot q)$ , where  $q \in \mathbb{R}^7$  is the costate vector. Let us consider the term  $C(r, q) := q_0 v_\rho + q_1 v_\theta + q_2 v_\psi + q_3 a_\rho + q_4 a_\theta + q_5 a_\psi$ . Then we can write the Hamiltonian as follows

$$H(r, t_f, q) := -t_f \min_{u \in \mathcal{U}} \left( \frac{T}{m} (q_3 \cdot \cos \alpha + \sin \alpha (q_4 \cdot \sin \delta + q_5 \cdot \cos \delta)) - q_6 \cdot \frac{T}{v_{\text{exhaust}}} \right) - t_f \cdot C(r, q).$$

As  $T$  is always positive, we can minimize the term  $(q_3 \cdot \cos \alpha + \sin \alpha (q_4 \cdot \sin \delta + q_5 \cdot \cos \delta))$  separately. We can rewrite the trigonometric functions  $a \cos x + b \sin x$  to  $R \cos(x - \arctan \frac{b}{a})$  with  $R = \sqrt{a^2 + b^2}$ . We, therefore, introduce the auxiliary variables  $\chi(\delta) := \sqrt{q_4^2 + q_5^2} \cdot \cos(\delta - \arctan \frac{q_4}{q_5})$  and  $A(\delta) := \sqrt{q_3^2 + \chi(\delta)^2}$ . We can first optimize over  $\alpha$ , and subsequently over  $\delta$  (notice that this sequential minimization is exact since  $A(\delta) \geq 0$ )

$$\begin{aligned} & \min_{\alpha, \delta \in [-\pi, \pi] \times [-\frac{\pi}{2}, \frac{\pi}{2}]} (q_3 \cos \alpha + \sin \alpha (q_4 \sin \delta + q_5 \cos \delta)) \\ &= \min_{\delta \in [-\frac{\pi}{2}, \frac{\pi}{2}]} A(\delta) \cdot \min_{\alpha \in [-\pi, \pi]} \cos(\alpha - \arctan \frac{\chi(\delta)}{q_3}). \end{aligned}$$

This results in the optimal thrust angles  $\alpha^*(\delta) := \pi + \arctan \frac{\chi(\delta)}{q_3}$ . Since  $\cos(\alpha^*(\delta) - \arctan \frac{\chi(\delta)}{q_3}) = -1$ , after applying  $\alpha^*(\delta)$ , it follows that  $\delta^* := \arg \min_{\delta \in [-\frac{\pi}{2}, \frac{\pi}{2}]} -A(\delta) = \arctan \frac{q_4}{q_5} \pm \pi$ . Subsequently, since  $\sqrt{q_3^2 + q_4^2 + q_5^2} \geq A(\delta)$ ,

$$q_3 \cos \alpha^* + \sin \alpha^* (q_4 \sin \delta^* + q_5 \cos \delta^*) = -\sqrt{q_3^2 + q_4^2 + q_5^2}. \quad (\text{IV.2})$$

The results of (IV.2) allow us to minimize with respect  $T$ , i.e.

$$\begin{aligned} H(r, t_f, q) &= -t_f \min_{T \in [0, T_{\max}]} \left( -\frac{T}{m} \cdot \sqrt{q_3^2 + q_4^2 + q_5^2} - q_6 \cdot \frac{T}{v_{\text{exhaust}}} \right) - t_f \cdot C(r, q) \\ \Rightarrow T^* &:= \begin{cases} T_{\max} & \text{if } \frac{q_6}{v_{\text{exhaust}}} + \frac{\sqrt{q_3^2 + q_4^2 + q_5^2}}{m} \geq 0 \\ 0 & \text{otherwise} \end{cases}. \end{aligned}$$

Finally, applying  $T^*$  and substituting  $-\min(\cdot)$  for  $\max(\cdot)$ , the Hamiltonian becomes

$$H(r, t_f, q) := -t_f \cdot C(r, q) + t_f \max \left( q_6 \cdot \frac{T_{\max}}{v_{\text{exhaust}}} + \frac{T_{\max}}{m} \sqrt{q_3^2 + q_4^2 + q_5^2}, 0 \right).$$

As in [6], we can use this simplified expression of the Hamiltonian to achieve significant computational savings when computing  $\omega$ . For a discussion of the convergence of  $\omega$  and the derivation of a necessary Courant-Friedrichs-Lewy condition, we refer to [22] and [19], respectively.

## B. Optimal trajectory reconstruction

The optimal control policy and trajectory  $(\mathbf{r}, \mathbf{u}) \in \Pi_{r_0, t_f}^{\mathcal{K}, \mathcal{C}}$  can be constructed efficiently using the approximation of  $\omega$  over  $\mathcal{G}$ . For a given  $N \in \mathbb{N}$  we consider the timestep  $h = \frac{1}{N}$  and a uniform grid with spacing  $s^k = \frac{k}{N}$  of  $[0, 1]$ . Let us define the state  $(r^k)_{k=0, \dots, N}$  and control  $(u^k)_{k=0, \dots, N-1}$  for the numerical approximation of the optimal trajectory and control policy. Setting  $r_0$  as the initial orbit and choosing an appropriate  $z$ , we determine  $\arg \min_{t_f} \omega(s^0, r_0, z, t_f)$  to find a corresponding  $t_f$ . We then proceed by iteratively computing the control value

$$u^k(r^k) = \arg \min_{u \in \mathcal{U}} \omega(s^k, r^k + h f(r^k, u, t_f), z, t_f) \bigvee g(r^k).$$

For a given  $\omega(s^k, r^k, z, t_f)$  this is done by numerically taking the partial derivatives along each grid direction to estimate the costate vector  $q$  and then determining the optimal control value as the minimizer of the Hamiltonian  $H$ . After  $u^k$  is determined we compute  $r^{k+1}$  using an appropriate Adams-Bashforth-Moulton method and increment  $k$ .

## C. Simulation results

To illustrate the theoretical results of the previous sections, we consider a spacecraft on an unstable initial orbit around asteroid Castalia 4769. The initial orbit spirals towards the asteroid and the spacecraft needs to make an orbit correction to a stable nominal target orbit so as to prevent a collision with the asteroid. The gravity of Castalia 4769 was modeled by means of a spherical harmonic expansion as discussed in [23].

For the numerical computation we considered the planar case, omitting the states  $\psi$  and  $v_\perp$ . The spacecraft is modeled with 1000 kg of dry mass, 100 N of maximum thrust and an exhaust velocity of 40 km/s. Using a target orbit with radius 6.1175 km and tangential velocity of  $-0.0025$  km/s as well as 0.2 kg of propellant, we are able to compute the numerical approximation of  $\omega$ . Following Theorem 3.1 and Theorem 3.3, any  $z$  that satisfies  $\min_{t_f} \omega(0, r_0, z, t_f) = \vartheta(r_0, z) = 0$  must belong to the set  $\Sigma_{r_0}$ . Using an initial orbit with radius 6.11 km and tangential velocity of  $-0.0026$  km/s, we are able to compute  $\Sigma_{r_0}$  by plotting the zero level set of  $\vartheta(r_0, z)$ , as shown in Fig. 1. Taking an arbitrary  $z$  from  $\Sigma_{r_0}$  and finding the minimal optimal time  $t_f = \arg \min_{t_f} \omega(0, r_0, z, t_f)$ , we are able to construct the optimal trajectory as described in Section IV-B and shown in Fig. 2.

## V. CONCLUSION

An approach to solving infinite and finite horizon multi-objective minimum time optimization problems was presented. Furthermore, we proved that strong and weak Pareto optimal values can be efficiently constructed from the zero level set of the unique viscosity solution of a Hamilton-Jacobi-Bellman equation. The feasibility and effectiveness of the proposed approach was demonstrated by applying it to the problem of low-thrust trajectory design. Future research concentrates towards constructing approximations of the reachable set and decomposing the optimization parameters

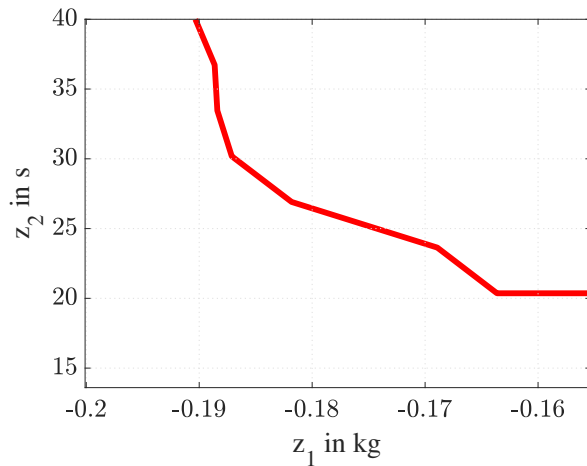


Fig. 1.  $\Sigma_{r_0}$  constructed from the zero level set of  $\vartheta$ .

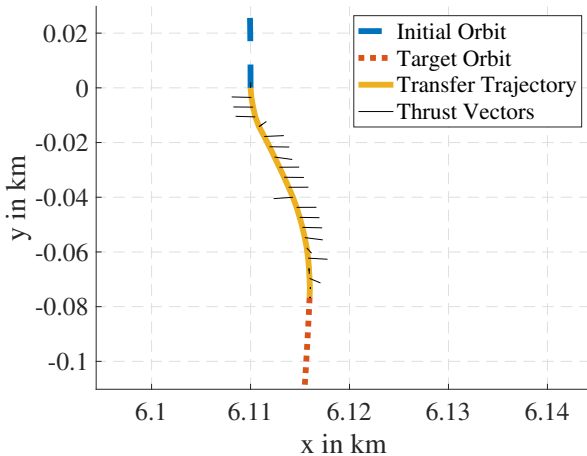


Fig. 2. The initial orbit is given by the dashed line, the optimal transfer trajectory (corresponding to the  $z$  pair  $[-0.18, 26.9]$ ) is reconstructed as described in IV-B and is given by the solid line, and the final orbit after the transition is complete is shown by the dotted line. The direction and magnitude of the continuous thrust is represented by the discretized set of solid lines shown along the transfer trajectory.

efficiently, so as to allow higher accuracy and computational efficiency.

#### ACKNOWLEDGMENT

We would like to thank Professor Bokanowski for correspondence on the numerical implementation. Furthermore, the authors would like to acknowledge the use of the University of Oxford Advanced Research Computing (ARC) facility in carrying out this work. <http://dx.doi.org/10.5281/zenodo.22558>

#### REFERENCES

[1] J. P. Aubin, J. Lygeros, M. Quincampoix, S. Sastry, and N. Seube, "Impulse differential inclusions: A viability approach to hybrid systems," *IEEE Transactions on Automatic Control*, vol. 47, no. 1, pp. 2–20, 2002.

[2] J. Lygeros, C. Tomlin, and S. Sastry, "Controllers for reachability specifications for hybrid systems," *Automatica*, vol. 35, no. 3, pp. 349–370, 1999.

[3] K. Margellos and J. Lygeros, "Hamilton-jacobi formulation for reach-avoid differential games," *IEEE Transactions on Automatic Control*, vol. 56, no. 8, pp. 1849–1861, aug 2011.

[4] —, "Toward 4-D trajectory management in air traffic control: A study based on monte carlo simulation and reachability analysis," *IEEE Transactions on Control Systems Technology*, vol. 21, no. 5, pp. 1820–1833, 2013.

[5] O. Bokanowski, E. Bourgeois, A. Désilles, and H. Zidani, "Payload optimization for multi-stage launchers using HJB approach and application to a SSO mission," *IFAC-PapersOnLine*, vol. 50, no. 1, pp. 2904–2910, 2017.

[6] O. Bokanowski, E. Bourgeois, A. Désilles, and H. Zidani, "Global optimization approach for the climbing problem of multi-stage launchers," Feb. 2015, working paper or preprint. [Online]. Available: <https://hal-ensta-paris.archives-ouvertes.fr/hal-01113819>

[7] J. F. Fisac, M. Chen, C. J. Tomlin, and S. S. Sastry, "Reach-avoid problems with time-varying dynamics, targets and constraints," in *Proceedings of the 18th International Conference on Hybrid Systems: Computation and Control*, ser. HSCC '15. New York, NY, USA: Association for Computing Machinery, 2015, p. 11–20.

[8] A. Désilles and H. Zidani, "Pareto front characterization for multi-objective optimal control problems using Hamilton-Jacobi approach," *SIAM Journal on Control and Optimization*, vol. 57, no. 6, pp. 3884–3910, 2019.

[9] S. Ober-Blöbaum, M. Ringkamp, and G. zum Felde, "Solving multiobjective optimal control problems in space mission design using discrete mechanics and reference point techniques," in *2012 IEEE 51st IEEE Conference on Decision and Control (CDC)*, 2012, pp. 5711–5716.

[10] D. C. Redding and J. V. Breakwell, "Optimal low-thrust transfers to synchronous orbit," *Journal of Guidance, Control, and Dynamics*, vol. 7, no. 2, pp. 148–155, 1984.

[11] N. Vertovec, S. Ober-Blöbaum, and K. Margellos, "Multi-objective minimum time optimal control for low-thrust trajectory design," 2021. [Online]. Available: <https://arxiv.org/abs/2103.08813>

[12] Y. Jiang and H. Baoyin, "Orbital Mechanics near a Rotating Asteroid," *Journal of Astrophysics and Astronomy*, 2014.

[13] D. T. Greenwood, *Principles of dynamics*, 2nd ed. Englewood Cliffs, N.J: Prentice-Hall, 1988.

[14] D. Liberzon, *Calculus of variations and optimal control theory: A concise introduction*. Princeton University Press, 2011.

[15] K. Miettinen, *Nonlinear Multiobjective Optimization*, ser. International Series in Operations Research & Management Science. Boston, MA: Springer US, 1998, vol. 12. [Online]. Available: <http://link.springer.com/10.1007/978-1-4615-5563-6>

[16] W. Dahmen and A. Reusken, *Numerik für Ingenieure und Naturwissenschaftler*. Springer, 2008.

[17] M. Bardi and I. Capuzzo-Dolcetta, *Optimal Control and Viscosity Solutions of Hamilton-Jacobi-Bellman Equations*. Birkhäuser Boston, 1997.

[18] M. Chen, S. L. Herbert, M. S. Vashishtha, S. Bansal, and C. J. Tomlin, "Decomposition of Reachable Sets and Tubes for a Class of Nonlinear Systems," *IEEE Transactions on Automatic Control*, vol. 63, no. 11, 2018.

[19] I. M. Mitchell, "The flexible, extensible and efficient toolbox of level set methods," *Journal of Scientific Computing*, vol. 35, no. 2-3, pp. 300–329, 2008.

[20] S. Bansal, M. Chen, S. Herbert, and C. J. Tomlin, "Hamilton-jacobi reachability: A brief overview and recent advances," in *2017 IEEE 56th Annual Conference on Decision and Control, CDC 2017*, 2018.

[21] S. Osher and R. Fedkiw, *Level Set Methods and Dynamic Implicit Surfaces*, ser. Applied Mathematical Sciences. Springer New York, 2003.

[22] O. Bokanowski, N. Forcadel, and H. Zidani, "Reachability and minimal times for state constrained nonlinear problems without any controllability assumption," *SIAM Journal on Control and Optimization*, vol. 48, no. 7, pp. pp. 4292–4316, 2010.

[23] D. J. Scheeres, S. J. Ostro, R. S. Hudson, and R. A. Werner, "Orbits close to asteroid 4769 Castalia," *Icarus*, vol. 121, no. 1, pp. 67–87, 1996.